Figure S1. Different types of chromosomal aberrations. Microscopic images illustrating chromosomes during mitosis with different types of CTAs and CSAs along with the schemes of their structure. Representative images of (A) chromatid exchange, (B) dicentric chromosome with its difragment and chromatid break, (C) abnormal chromosome, (D) three ring chromosomes with their difragments and (E) mitosis with several chromatid breaks. CSAs, chromosome-type aberrations; CTAs, chromatid-type aberrations.

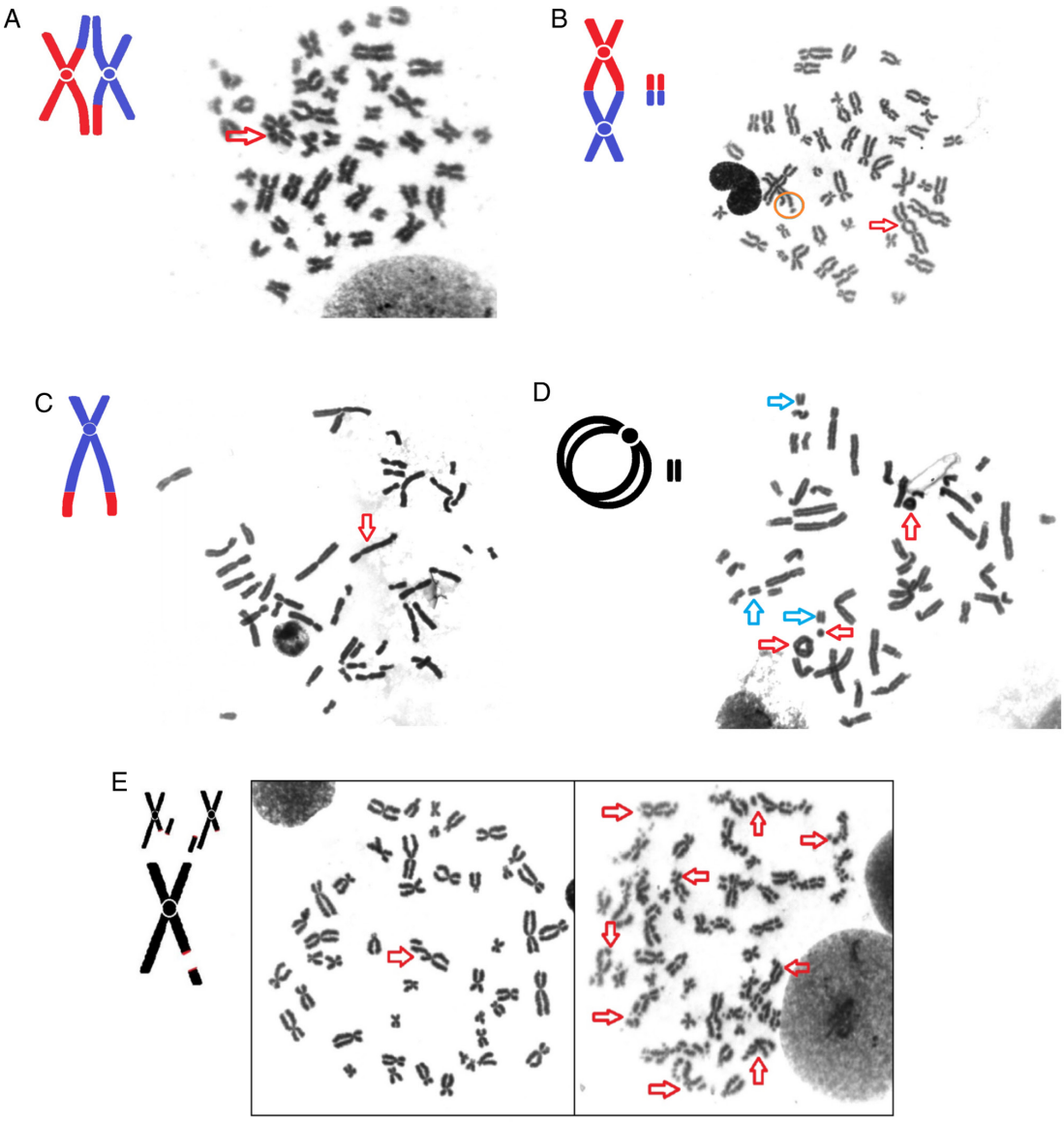

Figure S2. Results from relative telomere length measurements using monochrome multiplex real-time qPCR on a Viia 7 Real-time PCR System. (A) Representative calibration curve generated by performing serial dilutions of telomere standard. (B) Telomere amplification curve of two randomly selected samples. (C) Melt curve plot illustrating two specific products of the reaction, namely telomeres and albumin. (D) Albumin amplification curve of two randomly selected samples.

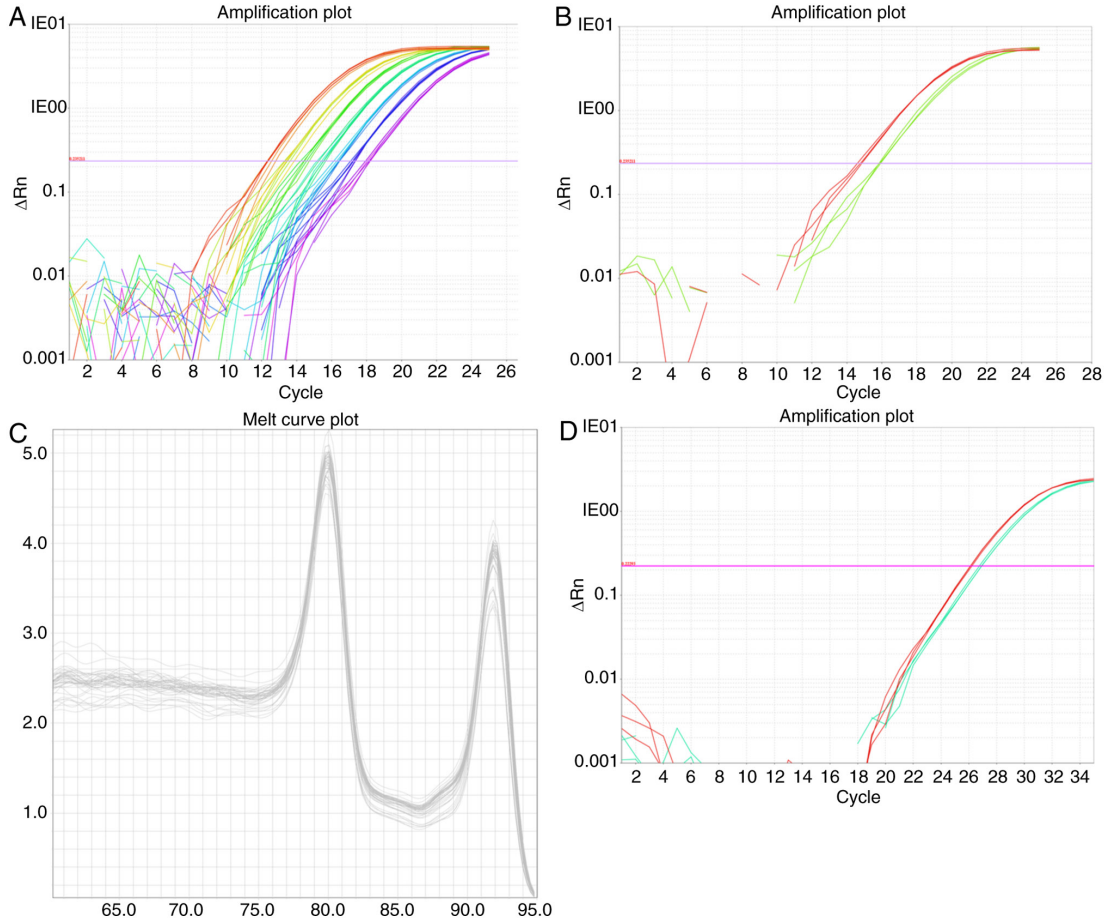

Figure S3. Spearman's rank correlation coefficient analysis between ACs, CAtot, CTAs and CSAs and TL. The correlation between ACs/CAtot/CTAs/CSAs and TL were investigated for (A) control individuals and patients with (B) BC, (C) CRC and (D) LC using Spearman's rank correlation coefficient analysis, which is expressed by the rs value and graphically plotted by linear regression. CA frequencies are presented on the x-axis, while the value of TL is presented as the RTL on the y-axis. Graphs from left to right: ACs, CAtot, CTAs, CSAs. CA, chromosome aberration; ACs, aberrant cells; BC, breast cancer; CAtot, total chromosomal aberrations; CRC, colorectal cancer; CSAs, chromosome-type aberrations; CTAs, chromatid-type aberrations; LC, lung cancer patients; RTL, relative telomere length; TL, telomere length.